

## Using Fluorescence Measurements to Model Key Phenomena in Microalgae Photosynthetic Mechanisms

Andrea Bernardi<sup>a</sup>, Andreas Nikolaou<sup>b</sup>, Andrea Meneghesso<sup>c</sup>, Tomas Morosinotto<sup>c</sup>, Benoit Chachuat<sup>b</sup>, Fabrizio Bezzo<sup>\*a</sup>

<sup>a</sup> CAPE-Lab: Computer-Aided Process Engineering Laboratory and PAR-Lab: Padova Algae Research Laboratory, Department of Industrial Engineering, University of Padova, Italy

<sup>b</sup> Centre for Process Systems Engineering, Department of Chemical Engineering, Imperial College, London, UK

<sup>c</sup> PAR-Lab: Padova Algae Research Laboratory, Department of Biology, University of Padova, Italy  
[fabrizio.bezzo@unipd.it](mailto:fabrizio.bezzo@unipd.it)

Fluorescence is a powerful tool in characterizing the photosynthetic properties of microalgae. In this work we discuss a dynamic model able to accurately represent Pulse Amplitude Method (PAM) fluorescence data. The model includes photoproduction, photoinhibition and photoregulation and has been calibrated using data from a culture of *Nannochloropsis Gaditana*. The main objective of the work is to propose an experiment design approach to determine information rich PAM experiments and identify the model. Moreover, we will show how the model can be used to predict the photosynthesis rate under dynamic light conditions. Finally, the work shows that different PI curve characteristics arise as a result of different experimental protocols and highlights the importance of the accurate description of the protocols used to derive the experimental data.

### 1. Introduction

Microalgae have long been identified a promising candidate for biofuel production in the transport sector (Chisti, 2007). The main advantages of microalgae with respect to other possible feedstock are the high potential productivity and the absence of competition with traditional crops for arable land. However, algae production on large scale is far from being profitable. Several issues need to be addressed to reach this objective, ranging from high nutrient requirement, the trade-off between biomass growth and lipid productivity, and lipid extraction (Mata et al., 2010).

In this context, the development of reliable models that are capable of predicting the behaviour of a microalgae culture accurately would be greatly beneficial. The possibility to represent the fundamental physical, chemical, and biological phenomena would allow to assess the interactions between equipment design and product yields and to scale-up and optimise the process design and operation. Microalgae exhibit a remarkable biological complexity due to the interaction of light and nutrient dependencies that span multiple time scales, ranging from milliseconds to days: photoproduction encompasses all the processes from photons utilization to CO<sub>2</sub> fixation that occur within milliseconds; photoinhibition, the observed loss of photosynthetic production due to excess or prolonged exposure to light, acts on a time scale of minutes to hours; photoregulation, also referred to as Non Photochemical Quenching (NPQ), the set of mechanisms by which microalgae protect their photosynthetically-active components via the dissipation of excess energy as heat, occurs within minutes; Photoacclimation, the ability of the cells to adjust their pigment content and composition under varying light and nutrient conditions, occurs within hours or days. Finally, the mechanisms involved in nutrient internalization and their metabolism into useful products occurs within hours or days as well (Falkowski and Raven, 1997).

Chlorophyll fluorescence is a powerful tool for the analysis of the aforementioned processes. Among others, Pulse Amplitude Modulation (PAM) equipment can implement complex protocols with great measurement accuracy. In this work we will present a dynamic model able to represent the main biological processes involved in fluorescence. We will use to calibrate the model data of the species *Nannochloropsis Gaditana*, an

alga of industrial interest because of the high growth rate and the ability to accumulate large amount of lipids. Furthermore, it has recently been selected for biotechnological genetic manipulations (Perin et al. 2014).

The first objective of this work is to determine a PAM protocol that contain the maximum information possible and allow for an accurate estimation of the uncertain model parameters using a Model-based design of experiment (MBDoe) approach (Franceschini and Macchietto, 2008). The second objective of the work is to show how the model can be used to predict Photosynthesis-Irradiance (PI) response curves. PI curves representation in a deterministic manner has been an important challenge for many years, since both the effects of light and nutrients can be captured and optimal productivities of large scale production systems can be inferred (Bernard, 2011). The most usual approach in representing PI curves includes the usage of steady state assumptions. However, despite their simple form and handiness static models often fail to explain the complexity of bioprocess dynamics and interactions. Moreover, the experimental procedure used to obtain PI curves is time consuming and requires conditions that are very different from the growing conditions in the photobioreactors (e.g. no mixing and no CO<sub>2</sub> excess). Once validated our model can be used to predict PI curves from fast and accurate fluorescence measurements.

## 2. A dynamic model for chlorophyll fluorescence

This section presents the dynamic model of fluorescence. Only the main equations of the model will be presented, for a more complete discussion about the model see Nikolaou et al. (2014).

Among the available fluorescence techniques, the focus here is on Pulsed Amplitude Modulation (PAM). A PAM protocol consists of a sequence of light events that trigger various photosynthetic processes in a given solution sample containing microalgae. A weak modulated light, called measuring light, is used to evaluate the fluorescence independently from actinic light, that is used to excite the photosynthetic apparatus. A third light source, called saturating pulse, is a strong flashing light that acts in a very short time scale in order to close all the reaction centres without affecting NPQ and inhibition to evaluate the maximum fluorescence.

The dynamic model accounts for the photoproduction, photoregulation and photoinhibition. It is based on the Han model (Han, 2002) for the description of photoproduction and photoregulation, and proposes a semiempirical relationship to account for qE-quenching photoregulation process. The fluorescence flux measured by the PAM fluorometer is expressed as:

$$F = \frac{S_F \sigma}{1 + \eta_D + \bar{\eta}_{qE} \alpha + A \eta_P + C \eta_I} \quad (1)$$

where  $S_F$  is a scaling parameter that lumps all the terms that are constant for a given photoacclimation state (in particular  $S_F$  is proportional to the chlorophyll content,  $chl$ , of the sample);  $\sigma$  denotes the total cross section [ $\text{m}^2/\text{g}_{chl}$ ]; and  $(1 + \eta_D + \bar{\eta}_{qE} \alpha + A \eta_P + C \eta_I)^{-1}$  is the quantum yield of fluorescence,  $\Phi_f$  [-]. The quantum yield of fluorescence depends on: i) parameters  $\eta_P$ ,  $\eta_D$ ,  $\bar{\eta}_{qE}$ ,  $\eta_I$ , which represent, respectively, the rates of photoproduction, basal thermal decay in dark-adapted state, qE-quenching and quenching linked to photoinhibition, all relative to the rate of fluorescence; ii) variable  $\alpha$ , which represents the activity of qE-quenching; and iii)  $A$  and  $C$ , which are the fraction of open and inhibited reaction centres of the photosystem II (RCII), the physical entity responsible for the production of one O<sub>2</sub> molecule. If the active (non-inhibited) RCII are all open ( $A=1-C$ ),  $F$  is indicated as  $F_0$ , while if active RCII are all closed ( $A=0$ ),  $F$  is indicated as  $F_m$ .

The Han model assumes that the RCII can be in either one of three states, namely open ( $A$ ), closed ( $B$ ) or damaged ( $C$ ). The equations in the Han model describe the dynamics of the fractions of  $A$ ,  $B$  and  $C$  RCII in the chloroplasts:

$$\begin{aligned} A &= -I \sigma_{PS2} A + \frac{B}{\tau} \\ B &= I \sigma_{PS2} A - \frac{B}{\tau} + k_r C - k_d \sigma_{PS2} I B \\ C &= -k_r C + k_d \sigma_{PS2} I B \end{aligned} \quad (2)$$

where  $\sigma_{PS2}$  denotes the effective cross section of the photosystem 2 [ $\text{m}^2 \mu\text{E}^{-1}$ ];  $\tau$  the turnover time [ $\text{s}^{-1}$ ];  $k_d$  the damage rate constant [-]; and  $k_r$  the repair rate constant [ $\text{s}^{-1}$ ]. Moreover,  $A(t) + B(t) + C(t) = 1$  at all times. Photoproduction is described by the transition from  $A$  to  $B$ ; photoinhibition, on the other hand, corresponds

to the transition from  $B$  to  $C$ , while the reverse transition from  $C$  to  $B$  describes repair of the damaged RCII by enzymatic processes.

Following Falkowski and Raven (1997) the parameter  $\sigma$  is related to  $\sigma_{PS2}$  of the Han model as:

$$\sigma_{PS2} = \Phi_p^A \frac{\sigma}{N} \quad (3)$$

where  $N$  is the number of RCII [ $\mu\text{E}/\text{g}_{\text{chl}}$ ], which remains constant for a given photoacclimation state;  $\Phi_p^A$  is the quantum yield of photosynthesis of an open RCII equal to  $\eta_p(1 + \eta_D + \bar{\eta}_{qE}\alpha + \eta_p)^{-1}$ . The expression for fluorescence quantum yield in Eq. 1 and for the quantum yield of photosynthesis are derived based on the work of Huot and Babin (2010) and on the lake model for the antenna-RCII complex (Kramer et al., 2004). Finally the variable  $\alpha$  that represent the activity of qE-quenching is described as a first order process:

$$\dot{\alpha} = \xi(\alpha_{SS}(I) - \alpha), \quad \alpha_{SS}(I) = \frac{I^n}{I_{qE}^n + I^n} \quad (4)$$

where  $\xi$  [ $\text{s}^{-1}$ ] denotes the rate of NPQ adaptation and  $\alpha_{SS}$  is the reference activity function for qE. Based on preliminary experimental data we expressed  $\alpha_{SS}$  as a sigmoid (Hill) function of light intensity where  $I_{qE}$  [ $\mu\text{E}/\text{m}^2\text{s}$ ] represents the irradiance level at which half of the maximal qE activity is realised ( $\alpha_{SS} = 0.5$ ); and  $n$  [-] describes the sharpness of the transition.

### 3. PI curve extension

We can observe that the model does not require any additional extension to predict PI curves. This comes forward if we consider the most general definition of photosynthesis rate:

$$P = \sigma \Phi I \quad (5)$$

with  $\Phi$  the oxygen photosynthesis quantum yield [ $\text{mol}_{\text{O}_2}/\mu\text{E}$ ] and  $I$ , the light intensity [ $\mu\text{E}/\text{m}^2\text{s}$ ]. The aforementioned units, give dimensions for  $P$  in [ $\text{mol}_{\text{O}_2}/\text{g}_{\text{chl}} \text{s}$ ], which by definition is the chlorophyll specific photosynthesis rate, in terms of  $\text{O}_2$  production. The dynamic model of fluorescence predicts the value of the realised quantum yield of photosynthesis,  $\Phi_{PS2}$  [ $\text{mol e}^-/\mu\text{E}$ ] in terms of electrons delivered to RCII. From literature, it is known that  $\Phi_{PS2}$  is closely related to  $\Phi$  (Suggett et al., 2003). A stoichiometric coefficient that aligns the electrons delivered in RCII to the  $\text{O}_2$  produced there needs introducing. If we consider the water dissociation reaction in PSII ( $2 \text{H}_2\text{O} + 4 \text{e}^- \rightarrow \text{O}_2 + 4 \text{H}^+$ ), a theoretical minimum value of 4 mol  $\text{e}^-/\text{mol O}_2$  can be derived as conversion factor. The model can be further extended to account for photoacclimation aiming at predicting PI curves for different acclimation states but this is beyond the scope of the work. Here the discussion will focus on the effect of the experimental protocol on model identification and on the model capability to predict PI curves.

## 4. Results and discussion

In the first subsection the results of MBDoe will be presented and discussed for a sample acclimated at 100  $\mu\text{E}/\text{m}^2\text{s}$ . In the second subsection model predictive capability of PI curves will be discussed. In particular, the importance of considering the protocol used to perform PI curve measurements will be pointed out.

### 4.1 MBDoe results for the dynamic model of fluorescence

The experiment considered for model calibration refers to a sample of *Nannochloropsis Gaditana* acclimated at 100  $\mu\text{E}/\text{m}^2\text{s}$  and a constant variance has been assumed to represent measurement error. As discussed in Nikolaou et al. (2014) some of the parameters of the model have been fixed to a literature value, as they require specific experiments to be accurately estimated. Table 1 summarises the estimates of the parameters values as obtained by a parameter estimation in the case a standard (non-designed) PAM experiment is used. The confidence intervals and t-values are also reported in Table 1. Although, Figure 1a shows a very good agreement between experimental data and the model, from Table 1 it can be observed that the model is not accurately identified. Circles, squares and triangles represent  $F_m'$ ,  $F_0'$  and  $F'$  respectively. The shaded area represents the light profile.

Table 1: The first three columns report parameter values estimated using one standard (non-designed) PAM experiment along with 95% confidence interval and t-values. Reference t-value is 1.65. The last three columns report the parameter estimates, confidence intervals and t-values using an optimally designed experiment. Statistically unsatisfactory estimates are indicated by (\*).

Parameter	Par. Value	95% Conf.Int.	t-val	95%	Par. Value	95% Conf.Int.	t-val	95%
	Non designed experiment				Optimally designed experiment			
$\xi_F$	$5.76 \cdot 10^{-2}$	$1.38 \cdot 10^{-2}$	4.07		$5.64 \cdot 10^{-2}$	$5.34 \cdot 10^{-3}$	10.82	
$I_{qE}$	$8.13 \cdot 10^2$	$9.43 \cdot 10^1$	8.32		$9.49 \cdot 10^2$	$6.16 \cdot 10^1$	4.32	
$k_d$	$7.06 \cdot 10^{-7}$	$1.76 \cdot 10^{-6}$	0.48*		$8.19 \cdot 10^{-7}$	$3.31 \cdot 10^{-7}$	2.18	
$n$	$2.39 \cdot 10^0$	$2.31 \cdot 10^0$	10.71		$2.23 \cdot 10^0$	$1.74 \cdot 10^{-1}$	5.91	
$\eta_I$	$7.84 \cdot 10^1$	$1.21 \cdot 10^2$	0.49*		$6.36 \cdot 10^1$	$3.29 \cdot 10^1$	2.53	
$\bar{\eta}_{qE}$	$1.87 \cdot 10^1$	$1.79 \cdot 10^1$	7.89		$2.07 \cdot 10^1$	$1.16 \cdot 10^0$	6.84	
$\eta_p$	$1.12 \cdot 10^1$	$3.12 \cdot 10^{-1}$	28.05		$1.15 \cdot 10^1$	$3.08 \cdot 10^{-1}$	16.55	
$S_f$	$1.68 \cdot 10^0$	$2.82 \cdot 10^{-1}$	4.99		$1.55 \cdot 10^0$	$9.66 \cdot 10^{-2}$	6.07	
$\sigma$	$8.13 \cdot 10^{-1}$	$1.52 \cdot 10^{-1}$	4.99		$8.82 \cdot 10^{-1}$	$1.85 \cdot 10^{-1}$	6.19	

In fact, the parameter estimation is not satisfactory from a statistical point of view, as some parameters are characterized by large confidence intervals (and low t-values). In particular, parameters  $k_d$  and  $\eta_I$  have a t-value well below the reference t-value, thus suggesting a correlation between the two parameters. However, C dynamics as represented by the third equation in set (2), shows the importance of  $k_d$  at representing kinetics leading to damage in the reaction centres. It is therefore quite a significant parameter and a precise estimation is advocated for an accurate description of light induced inhibition.

Thus, in order to improve the precision of parameter estimation and to identify the model a MBDoE has been performed. The design is based on the A-criterion and aims at optimising a PAM protocol with 20 light steps and 50 measurements. The optimisation determines the light intensity of each light step and the measuring points (i.e. the time at which a saturating pulse is applied). The minimum time gap between two measurement has been set to 40 s in order to assure the validity of the biological assumption that the saturating pulses do not affect photoinhibition and photoregulation. In Figure 1b the optimal experiment is reported along with the simulated measurements.

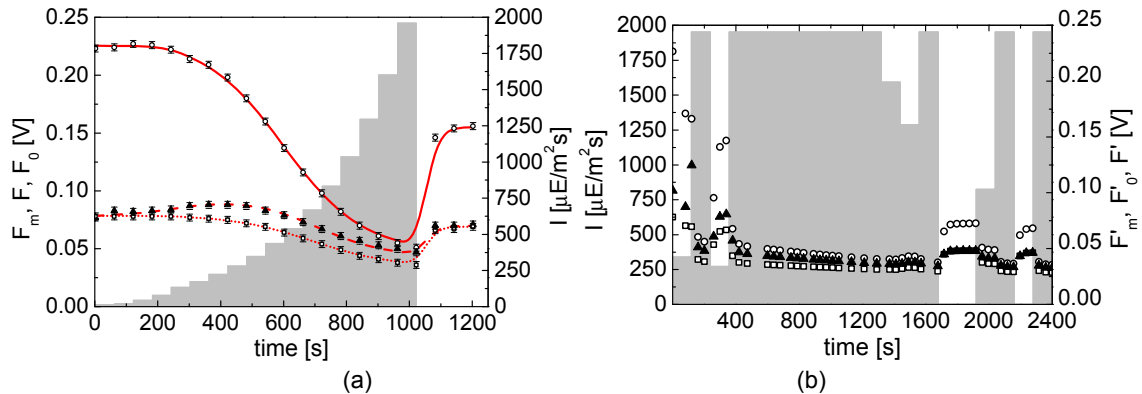


Figure 1: Model calibration results along with experimental data (a) and optimally designed experiment along with predicted data points (b) for a sample acclimated to 100  $\mu E/m^2 s$ .

The last three columns of Table 1 report the newly estimated values of the parameters, the confidence intervals, and t-values after the designed experiment. The results show that a confident parameter estimation

can be achieved through the utilisation of MBD<sub>oE</sub>. It is important to underline that measurement noise or model mismatch can hinder the practical identifiability and future work will include the experimental validation of the suggested procedure.

#### 4.2 PI curve prediction

Once validated the model will be suitable for prediction of photosynthesis rate based on the formulation reported in Section 3. In order to predict a PI response curve we can simulate an *in silico* experiment. In the following we will compare two different experimental set up. In the first experimental set up, indicated as Type A, we consider that to determine an experimental point a sample of the culture has to be kept at constant light for a certain amount of time, called incubation time, before measuring the value of  $P$ . The second experimental set up, indicated as Type B, considers to have only one sample exposed to a varying light intensity. The light will follow a step profile with the light increasing from zero to a maximum value and  $P$  will be measured at the end of each constant light step. Note that in the literature PI curves data are, in majority, reported without the experimental protocol that was used to obtain them. We will show how dynamic modelling plays a crucial role and the experimental protocol can lead to different PI curves behaviour.

The experiment that we are considering are simulated experiments obtained with the model calibrated in the previous section. Figure 2a compares the Type A and Type B experiments. For each experimental set up two alternatives are considered regarding the duration of the experiment. The dotted and the dashed line refers to Type A experiment. Ten samples are assumed to be exposed independently to ten different light intensities ranging from 0 to 2000  $\mu\text{E}/\text{m}^2\text{s}$ . The incubation time has been set to 1800 s for the dotted line and to 3600 s for the dashed line. The continuous line and the dot-dash line refers to Type B experiment. The irradiance is assumed to increase from 0 to 2000  $\mu\text{E}/\text{m}^2\text{s}$  following a step profile with ten constant light steps. Each step lasts 300 s for the continuous line and 600 s for the dash-dot line; at the end of each step  $P$  is measured and the light is increased by 200  $\mu\text{E}/\text{m}^2\text{s}$ . Figure 2b investigates the effect of the initial condition of damage in the predicted profile if a Type B experiment is considered (Type A results lead to equivalent conclusions). The three curves of Figure 2b consider a step duration of 300 s. The continuous line is the same as in Figure 2a, while the dashed line considers an initial value of  $C$  (i.e.  $C_0$ ) equal to 0.1 whereas the dotted line considers  $C_0$  equal to 0.2.

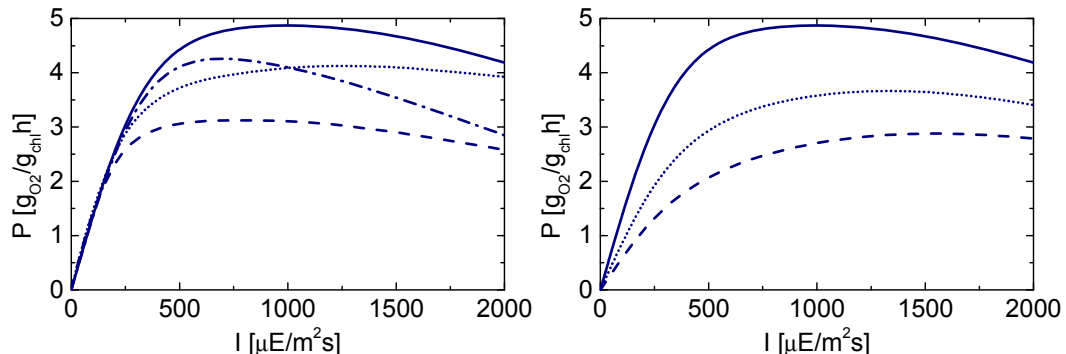


Figure 2: (a) PI curves for a sample acclimated at 100  $\mu\text{E}/\text{m}^2\text{s}$  and different light protocols. (b) PI curves obtained for a Type B experiment with 300 s constant light step and different initial conditions.

From Figure 2a we can observe how both the experimental set up and duration affect the PI curves. The type of experiment affects the shape of the PI curves, while the initial slope remain constant. Note that the experiment duration affects the behaviour of PI curves at high light intensities. In fact, a longer experiment will cause an higher amount of photoinhibition at high light intensities, thus leading to diminished photosynthetic production. From Figure 2b we can observe that, if at the beginning of the protocol the sample has a certain amount of inhibited reaction centres, we have a reduction both on the initial slope and on the maximum photosynthesis rate. In view of the above, it can conclude that it is necessary to consider a dynamic model and that the exact experimental protocol used to obtain the PI curves should be taken into account, if misleading conclusions or wrong parameter estimation are to be avoided. Also the initial condition of damage needs to be evaluated in order to correctly compare different PI curves. This is particularly important if we consider cells acclimated at high light conditions, where an initial damage is likely to be present as consequence of the stressful growing environment.

## 5. Conclusion

A model representing the main biological processes related to photosynthetic production has been presented and discussed. A semi-mechanistic representation of the photoproduction, photoregulation and photoinhibition phenomena has been developed. The opportunity to use a MBDoE approach to increase the accuracy of parameter estimation and assure the model identifiability has been discussed. An optimally designed experiment has been determined and will have to be carried out in order to confirm the practical identifiability of the model. The model well represents the available experimental fluorescence data and is able to predict PI-irradiance response curves based only on fluorescence measurements. Once validated the model will allow to predict PI curves using fast and reliable fluorescence measurement, instead of performing a time consuming and inaccurate PI curve protocol. Finally, simulation results underline that is extremely important for the utilization of PI curves in estimation of biomass productivity to specify the exact protocol followed to perform the measurements and the initial condition of the photosynthetic apparatus.

## Acknowledgements

AN and BC gratefully acknowledge financial support by ERC career integration grant PCIG09-GA-2011-293953 (DOP-ECOS). TM gratefully acknowledges financial support by ERC starting grant 309485 (BIOLEAP). AB and FB gratefully acknowledge Fondazione Cariparo for grant Progetto Dottorati di Ricerca 2012. FB and TM gratefully acknowledge financial support by project PRIN 2012 prot. 2012XSAWYM "Improving biofuels and high added value molecules production from unicellular algae".

## References

- Bernard O., 2011. Hurdles and challenges for modelling and control of microalgae for CO<sub>2</sub> mitigation and biofuel production. *Journal of Process Control* 21, 1378–1389.
- Chisti Y., 2007. Biodiesel from microalgae. *Biotechnology Advances* 25, 294–306.
- Falkowski P.G., Raven J.A., 1997. Aquatic photosynthesis. Vol. 256. Blackwell Science Malden, MA.
- Franceschini G., Macchietto S., 2008 Model-based design of experiments for parameter precision: State of the art. *Chem. Eng. Sci.* 63, 4846–4872
- Han B.P., 2002. A mechanistic model of algal photoinhibition induced by photodamage to photosystem-II. *Journal of Theoretical Biology* 214, 519–27.
- Huot Y., Babin M., 2010. Overview of fluorescence protocols: theory, basic concepts, and practice. Book Chapter. In: *Chlorophyll a Fluorescence in Aquatic Sciences: Methods and Applications* (D.J. Suggett, O. Prášil, M. A. Borowitzka, Eds.). *Developments in Applied Phycology* 4. Springer The Netherlands, pp. 31–74.
- Kramer D., Johnson G., Kiirats O., Edwards G., 2004. New fluorescence parameters for the determination of q(a) redox state and excitation energy fluxes. *Photosynthesis Research* 79, 1209–218.
- Mata T.M., Martins A.A., Caetano N.S., 2010. Microalgae for biodiesel production and other applications: a review. *Renewable and Sustainable Energy Reviews* 14, 217–232.
- Nikolaou A., Bernardi A., Meneghesso A., Bezzo F., Morosinotto T., Chachuat B., 2015. A model of chlorophyll fluorescence in microalgae integrating photoproduction, photoinhibition and photoregulation. *Journal of Biotechnology* 194, 91–99.
- Perin G., Segalla A., Basso S., Simionato D., Meneghesso A., Sforza E., Bertucco A., Morosinotto T., 2014. Biotechnological optimization of light use efficiency in nanochloropsis cultures for biodiesel production. *Chemical Engineering Transactions* 37, 763–768.
- Suggett D.J., Oxborough K., Baker N.R., MacIntyre H.L., Kana T.M., Geider R.J., 2003. Fast repetition rate and pulse amplitude modulation chlorophyll a fluorescence measurements for assessment of photosynthetic electron transport in marine phytoplankton. *European Journal of Phycology* 38, 371–384.